Organic Electronics 13 (2012) 1456–1462

Contents lists available at SciVerse ScienceDirect

Organic Electronics

journal homepage: www.elsevier.com/locate/orgel

Charge trapping and electroluminescence at quantum dots embedded in a polymer matrix

Dhirendra K. Sinha [a,b], Yashowanta N. Mohapatra [a,b,c,*]

[a] Department of Physics, Indian Institute of Technology Kanpur, Kanpur 208016, India
[b] Samtel Centre for Display Technologies, Indian Institute of Technology Kanpur, Kanpur 208016, India
[c] Material Science Programme, Indian Institute of Technology Kanpur, Kanpur 208016, India

ARTICLE INFO

Article history:
Received 17 February 2012
Received in revised form 3 April 2012
Accepted 20 April 2012
Available online 4 May 2012

Keywords:
Quantum dots
Polymers
Photoluminescence
Electroluminescence
Traps

ABSTRACT

We unambiguously demonstrate that mechanisms of photoluminescence (PL) and electroluminescence (EL) are different for CdSe/ZnS quantum dots (QDs) embedded in a polymer host. With increase in concentration of QDs, EL intensity increases exponentially when the impressed current is kept the same. In contrast, PL intensity shows only a linear dependence on the concentration of quantum dots. In the case of EL, the QDs of 3.2 nm diameter act as giant centers with a nearly temperature independent capture cross-section in the temperature range of 10–300 K. A phenomenological model of carrier capture is proposed in which the hole capture cross-section is exponentially distributed due to non-uniform distribution of QD particles in the host. We also show that EL yield and effective carrier mobility (μ_{eff}) share identical non-Arrhenius temperature dependence for each concentration of embedded QDs. Possible origin of hole capture mechanisms are discussed in the light of these experimental observations.

1. Introduction

In the last two decades, the research on QD-polymer composites has emerged almost as a discipline due to their importance in a wide range of potential applications. The combination of the twin advantages of tailorability of properties of QDs and easy processability of polymers has led to their potential use in many applications of large area electronics including light emitting displays, solar cells, printable transistors and sensors [1,2].

There have been many different approaches in studying and optimizing luminescence of colloidal QDs in polymers. Colvin et al. [3] studied bilayer structure in which emission was attributed to the recombination of holes injected into a *p*-paraphenylene vinylene layer with electrons injected into a CdSe QD layer. Dabbousi et al. [4] reported EL from the blend of polyvinylcarbazole (PVK), electron functional species *t*-Bu-PBD, and CdSe QDs. In subsequent years, several groups explored the device performance utilising these two approaches [5] together with the use of core/shell QDs such as CdSe/ZnS [6], CdSe/CdS [7], and even efficient EL near infrared using InAs/ZnSe nanocrystals [8]. Coe et al. [9] studied the luminescence processes in a quantum dot light emitting diode (QD-LED) that contains only a monolayer of CdSe/ZnS QDs passivated with trioctylphosphine oxide and sandwiched between the hole and electron transporting organic thin films. Later, Anikeeva et al. [10] varied the location of an emissive QD monolayer within a QD-LED multilayer structure in order to investigate the electronic and excitonic processes. Recently, a field induced tunnelling mechanism is also proposed to explain EL [11]. Though the dynamics of exciton processes at QD have been studied through fast pump–probe experiments [12], the results have not been used to explain concentration and temperature dependence of steady state measurements effectively. A coherent and quantitative understanding of mechanism of EL is yet to emerge limiting their effective use.

* Corresponding author at: Department of Physics, Material Science Programme, Indian Institute of Technology Kanpur, Kanpur 208016, India. Tel.: +91 512 2597033/2597538.
E-mail address: ynm@iitk.ac.in (Y.N. Mohapatra).

1566-1199/$ - see front matter © 2012 Elsevier B.V. All rights reserved.
http://dx.doi.org/10.1016/j.orgel.2012.04.016

The proposed mechanisms of luminescence in the literature are mostly based on: (a) carrier recombination following direct charge injection into the QDs, (b) transfer of excitons from the host into QDs and subsequent recombination, or (c) a combined contribution from the two afore-mentioned processes [9,10,13–19]. In spite of many studies, the role of QDs in controlling the charge processes remains unclear due to lack of quantitative correlations over a wide range of QD concentration and temperature. Specifically, possible differences in mechanisms of PL in the material and EL in diodes based on QDs embedded polymer are not understood. PL intensity is known to increase on lowering the temperature ostensibly due to reduction in non-radiative recombination pathways [4], but the case of EL is unclear since both types of behavior have been reported [4,20].

In this article, we simultaneously study transport and luminescence processes in the well-known system consisting of core–shell CdSe/ZnS QDs embedded in the Poly[9,9-dioctylefluorenyl-2,7-diyl] (PFO) host matrix. The transport and EL were investigated in light emitting diode structures with a wide range of QD particle density in the temperature range of 10–300 K. Since it is known that the diode parameters change with concentration and temperature, it is extremely important to keep the processing conditions similar, and the excitation conditions, such as the impressed current density to be the same for all experiments being compared. Taking care of this precaution is a key factor that allows us to make a fair comparison of capture and recombination processes, and in reaching unambiguous conclusions and extracting quantitative parameters. The direct correlation between the charge transport and EL is observed demonstrating that in contrast to PL, EL involves capture of charge with QDs acting as traps with exponentially distributed capture cross-section.

2. Experimental methods

For the present study, we obtained colloidal CdSe/ZnS core–shell QDs of diameter 3.2 nm, band gap 2.12 eV, and uniformly dispersed in toluene having concentration 10 mg/ml from Evident Technologies. We used Poly[9,9-dioctylefluorenyl-2,7-diyl] end capped with dimethylphenyl as a host polymer (obtained from American Dye Source and abbreviated as PFO). Fig. 1(a) shows the structure of host polymer and schematic of a core–shell QD. In order to load the QDs into the host polymer, we first dissolve 10 mg of PFO in 1 ml of toluene solvent and stir it for 12 h at room temperature using magnetic stirrer. The PFO solution is then filtered using a filter paper of pore size 10 μm (Millipore). Finally, the composite solutions, prepared to get appropriate wt.% loading of QDs, are stirred for 1 h at room temperature to ensure uniform mixing. The device fabrication steps include the spinning of composite solutions at the optimized rate of 1000 rpm over the pixilated indium doped tin oxide (ITO) substrates, pre-coated with poly(3,4-ethylenedioxythiophene):poly(styrene sulfonate) PEDOT:PSS acting as a hole injecting layer. The solvent evaporation from active layer was carried out at 120 °C for

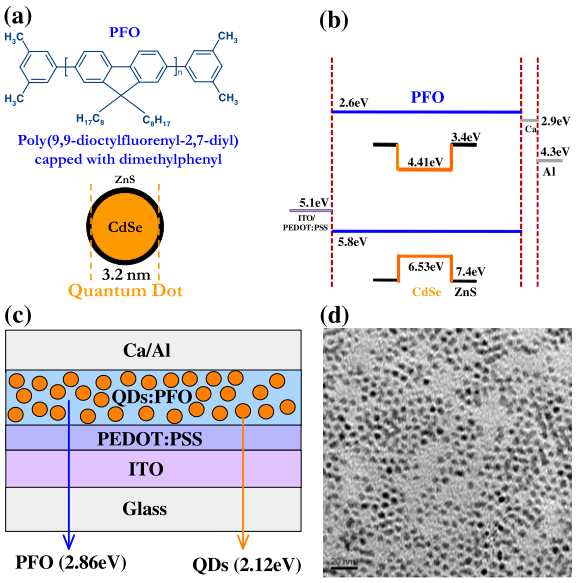

Fig. 1. (a) The molecular structure of host polymer and schematic of the CdSe/ZnS QDs, (b) energy level diagram of ITO|PEDOT:PSS|PFO:QDs|Ca|Al device, where all energies are indicated with respect to the vacuum level. (c) schematic of single layer device structure depicting the QDs embedded polymer layer sandwiched between ITO and Ca/Al electrodes. The EL peak energy corresponding to both QDs and PFO is indicated by arrows. (d) HR-TEM of 80 wt.% QD embedded polymer solution.

2 h under high vacuum. The cathode was formed by sequentially depositing calcium and aluminum by thermal evaporation over the active layer at a pressure of 10^{-6} mbar. The finished devices were sealed under nitrogen environment. The thickness of active layers was determined using profilometer (Tencor alpha–Step 500). The device was biased at a constant current of 1 mA using Keithley 2601 source measure unit and the EL spectrum was recorded using a spectro-radiometer (Minolta CS-1000A). The PL spectra were recorded with an excitation wavelength of 370 nm. The high resolution transmission electron micrograph (HR-TEM) was taken on a copper grid for composite solution with 1.34×10^{16} QDs/cm^3 in PFO. For mobility measurement using electroluminescence transients (ELT) a 50 MHz HP 81101A pulse generator, with a rise time of 10 ns, was used to apply rectangular voltage pulses of different magnitude and pulse width across the devices. The details of ELT measurement procedure and determination of fast carrier mobility have already been reported elsewhere [21]. For temperature dependent measurements, the device was mounted on the cold finger of a CTI closed-cycle cryostat and the temperature of the sample was maintained using Lakeshore 370 temperature controller.

3. Results and discussion

3.1. Concentration dependence

Fig. 1(b) shows the energy level diagram of the device, and the schematic of the device structure is shown in Fig. 1(c), where a 40 nm thin active layer which is a

composite of PFO and QDs, symbolically represented by bubbles dispersed in the background of polymer. We analytically estimate the QD particle density in the active area of the device. It turns out to be approximately $8.4 \times 10^{14}\,cm^{-3}$ for 20 wt.%, $3.3 \times 10^{15}\,cm^{-3}$ for 40 wt.%, $7.5 \times 10^{15}\,cm^{-3}$ for 60 wt.%, and $1.34 \times 10^{16}\,cm^{-3}$ for 80 wt.% QDs. Further, in order to ensure that the QDs are well dispersed as distinct entities without any agglomeration at a microscopic scale, we spread the composite solution over a copper grid, dry it and then observe it under HR-TEM. The micrograph, as depicted in Fig. 1(d) clearly indicates that QDs are randomly distributed in the host material without any agglomeration.

Fig. 2 shows the room temperature EL and PL spectra, normalized with respect to the PFO peak energy, for different loading concentration of QDs. It is important to note that for exciting EL, the biasing current was kept constant to ensure approximately the same level of charge injection in all the devices. This is the single most important precaution required to enable fair comparison between mechanisms across different devices. It is known that the contact potential is dependent on degree of loading [8], the choice of cathode [22], and changes with temperature [23]. Hence conclusions from experiments without keeping the current density constant can be misleading. In both EL and PL, the spectrum exhibits two spectrally separated regimes: the luminescence between 2.4 eV and 3 eV is from the PFO and the emission from QDs is centered at 2.12 eV. It may be significant to note here that the choice of the host and QD size has been deliberately such that the emission from QD can be monitored separately.

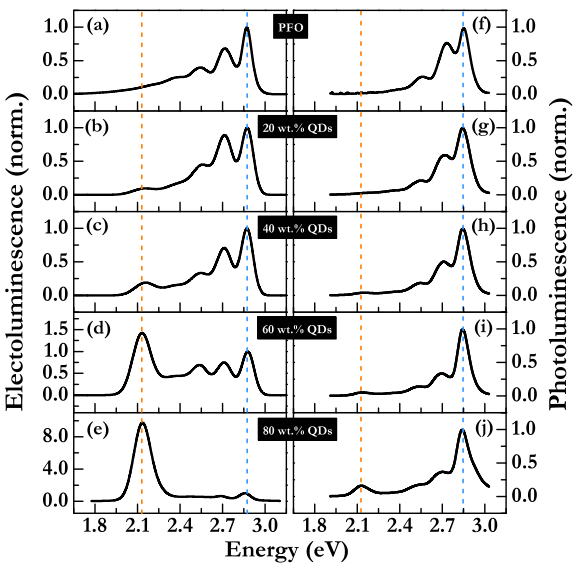

Fig. 2. (a)–(e) Room temperature EL spectrum of the devices with increasing concentration of QDs in the host PFO. The EL was recorded while the devices were biased at a constant current of 1 mA. (f)–(j) PL spectrum of the corresponding thin films on quartz substrates. For PL, the samples were excited with 370 nm source. The orange (blue) dash line marks the emission peak energy originating from the QDs (PFO). (For interpretation of the references to colour in this figure legend, the reader is referred to the web version of this article.)

In PL, the contribution to emission from QDs increases with concentration though it remains small in comparison to the peaks from the host. Fig. 3 is a plot of integrated area under the PL peak of QD emission as a function of QD concentration showing clearly the dependence to be linear. In contrast, the EL intensity from the QDs increases dramatically becoming the dominant peak at higher concentrations.

Fig. 4(a) shows integrated area under the EL peak of QD emission, which shows a sigmoidal shape in a linear plot. It can be fitted to a function of QD concentration N_{QD} where probability $P_{emission}$ is given by,

$$P_{emission}(N_{QD}) = \frac{1}{1 + \alpha e^{-V_c N_{QD}}}, \tag{1}$$

where V_c is the associated capture volume, and α is a parameter that can depend on trap kinetics. The function empirically presents itself as a cumulative distribution function of the usual logistic probability distribution. Capture models such as these are often used to test hypotheses in analogous, though more complicated, situations such as that of animal capture in the wild by setting up traps [24], or fish catch in nets and trawlers [25]. Specifically, the spatial distribution of traps plays a significant role in increasing the effective capture probability for the species to be captured taking into account its concentration, size and mobility through parameters of the logistic distribution. If the second term in the denominator in Eq. (1) is large the function can be approximated to an exponential. The parameter α does turn out to be large enough so that the functional dependence can be approximated to an exponential. The slope of the semi-log plot would then directly yield the co-efficient of distribution of the associated capture volume. Fig. 4(b) shows the increase in EL from QDs as a function concentration for three representative temperatures in a semi-log plot. Table 1 lists the capture co-efficient associated with volume distribution from both kinds of fit for different temperatures. For the exponential fit, the distribution co-efficient varies between $2.56 \times 10^{-10}\,cm^2$ and $2.11 \times 10^{-10}\,cm^2$, while it is slightly higher for the sigmoidal fit. The values indicate that the process is temperature independent. This is to be expected since the

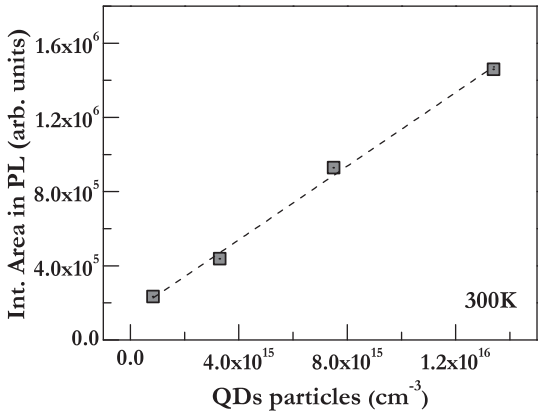

Fig. 3. Integrated area under the PL peak of QDs emission with increasing QD concentration. The dashed line is a linear fit to the data.

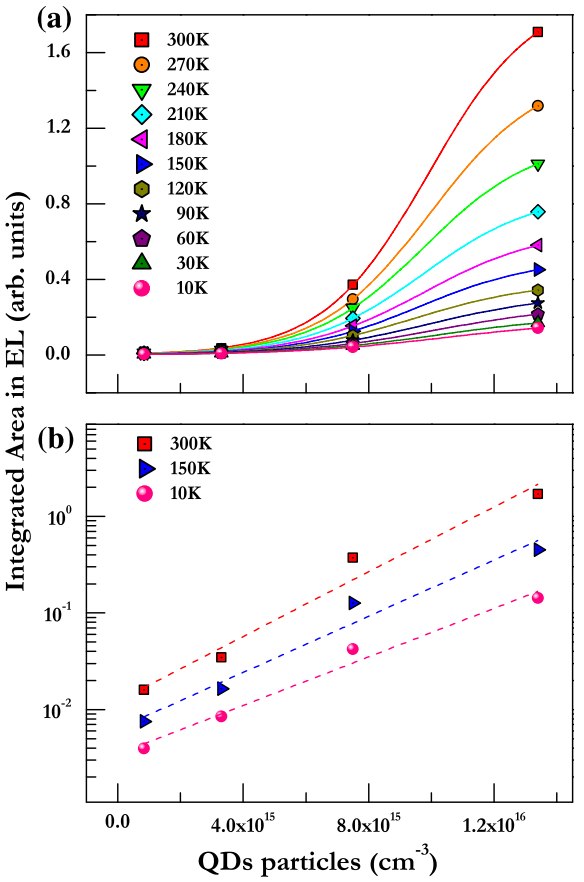

Fig. 4. (a) Integrated area under EL peak of QDs emission with increasing QD concentration in the temperature range of 10–300 K. The bold line is the sigmoidal fit to the data. (b) The same data plotted on a semi-log scale for three representative temperatures for clarity. The dashed lines are the linear fit of the data.

Table 1
Associated capture cross-section of the volume distribution as a function of temperature obtained from sigmoidal and exponential fit of concentration dependence of QD emission.

Temperature (K)	Exponential fit	Sigmoidal fit
	Capture cross-section (cm^2) $\times 10^{-10}$	
300	2.56	3.41
270	2.51	3.32
240	2.46	3.30
210	2.42	3.23
180	2.37	3.16
150	2.33	3.15
120	2.29	3.11
90	2.25	2.96
60	2.20	2.85
30	2.14	2.77
10	2.11	2.71

co-efficient arises from a geometrical distribution. In Section 3.3, we present a phenomenological model based on carrier capture dynamics leading to the observed concentration dependence.

3.2. EL and mobility: correlation in T-dependence

In order to investigate the mechanism of luminescence further, we measure the integrated area under QD emission in EL as a function of temperature, and compare it with temperature dependence of mobility for different amounts of QD loading. Fig. 5 shows simultaneous plots of mobility and QD emission as a function of inverse temperature for different amounts of loading. Clearly, the EL emission mimics the temperature dependence of mobility quite closely showing unambiguously that the recombination leading to EL is proportional to the carrier mobility, where the Langevin recombination rate constant γ is given by, $\gamma = e\mu_{eff}/\varepsilon$ where, e is the electronic charge, μ_{eff} is the effective charge mobility and ε is the permittivity.

It is also important to note from these results that mobility, for example, at room temperature decreases by a *factor* of 2 over the composition range. On the other hand, QD emission as shown in the last section increases over *two orders* of magnitude with concentration. Hence the observed QD concentration dependence cannot be explained on the basis of changes in effective mobility treating it to be a Langevin process.

In the present case, the recombination is dependent essentially on the hole mobility since PFO is a hole transporting material, and our EL transient results refer to the hole mobility. Further, if the mobile hole is recombining with an immobile electron at a trap, it is essentially the mobility of the hole that would control the rate determining step in the recombination. The temperature dependence of mobility in conjugated polymers is known to show non-Arrhenius behavior due to several reasons including the change of effective mobility gap within Gaussian DOS, the concentration dependence due to changes in occupation, and multiple trapping from deep and localized states [27–30]. We will discuss this in a separate article focused on transport in presence of QDs. Here it suffices to note that the EL intensity essentially follows the temperature dependence of carrier mobility when the injected current density is kept constant. Since it is dependent on the mobility, the QD must be getting charged by one of the carriers (electrons in this case), and then acting as an attractive charged recombination centre for the holes. The capture process is thus limited by carrier approach and not by any energy barrier at the interface between the QD and the medium, or by the ease of availability of phonon.

It is interesting to note that Kuik et al. [31] have argued in a recent paper along similar lines to suggest that the trap assisted recombination co-efficient is proportional to the hole mobility alone if the recombination occurs at the electron traps. The scenario described for red luminescence (in a white light emitting co-polymer) occurring due to recombination at an electron-trapping chromophor is similar to the mechanism being proposed here. From the trap assisted recombination assumption, they have derived capture coefficient at the traps from detailed fitting of the light intensity dependence of open circuit voltage V_{oc}. The mechanism proposed here is similar in the sense that recombination co-efficient in low-mobility materials is shown to be proportional to the capture cross-section since

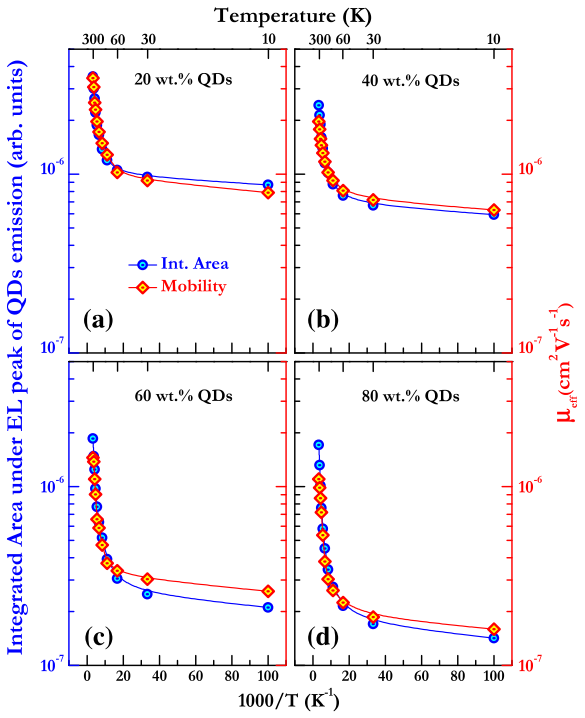

Fig. 5. Temperature dependent integrated area under EL peak of QDs emission (blue circle) and effective charge carrier mobility (red diamond) of the devices at similar biasing condition. The plots in four panels correspond to the different loading concentration of QDs into PFO, (a) 20 wt.% QDs, (b) 40 wt.% QDs, (c) 60 wt.% QDs, and (d) 80 wt.% QDs. In each case, the absolute value of integrated area is multiplied by an arbitrary factor in order to show it on the same scale of mobility values. The plots clearly indicate the direct dependence of the recombination rate to the effective charge carrier mobility in the devices. For more clarity, temperatures are indicated on the top *x*-axis. (For interpretation of the references to colour in this figure legend, the reader is referred to the web version of this article.)

the recombination is limited by the mobility of one of the carriers.

3.3. Phenomenological model: carrier trapping

We have already shown that mobility changes alone cannot be responsible for the observed dependence on QD concentration. It can be argued that while keeping the current density constant implies that the majority hole carrier concentration is approximately the same, the electron current component could be changing drastically with composition. If that were the case, one would have observed strong temperature dependence in emission as a function of composition. Recall that the phenomenological parameter within the exponential in Eq. (1) has already been shown to be nearly temperature independent. Hence an explanation based on carrier concentration is highly unlikely. We go on to propose a simple phenomenological model based on charge trapping.

Treating the electron and hole capture processes along the lines of Shockley–Read–Hall (SRH) model of deep levels in semiconductors [26], we represent the relevant capture processes in Fig. 6 with the traps in the band gap

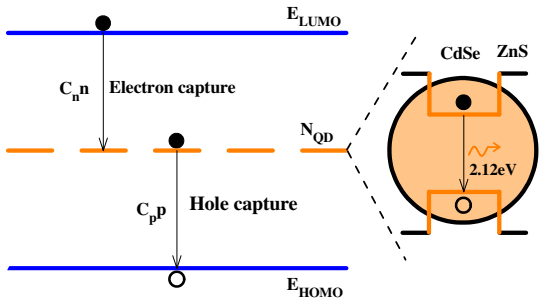

Fig. 6. Schematic of electron and hole capture transitions treating QD as a trapping center from which emission occurs when a negatively charged centers (of concentration n_T capture holes). The notations of transition arrows are consistent with the convention of showing electron jumps as is normally used in SRH model of defects in semiconductors.

representing the QD as shown. We ignore the thermal emission rates as they are negligible at the temperatures of interest due to large energy barrier. Also, the processes of interest occur during forward bias in presence of large concentration of carriers. Therefore, capture processes are assumed to be dominant over emission. Let n_T, p_T denote the concentration of QD trapping centers occupied with electrons and holes respectively, and emission at QD would occur on capture of a hole. The emission intensity at anytime would then be proportional to p_T. We write rate equation for p_T as,

$$\frac{dp_T}{dt} = C_p p(N_{QD} - p_T) - C_n n p_T, \tag{2}$$

where C_n and C_p are the capture coefficients of the electrons and holes, respectively. Here $C_p = \langle \nu_{th} \rangle_p \sigma_p$ and $C_n = \langle \nu_{th} \rangle_n \sigma_n$ where $\langle \nu_{th} \rangle_p$, $\langle \nu_{th} \rangle_n$ are the thermal emission rates of holes and electrons and σ_p, σ_n are the respective capture cross-sections. In the steady state condition $\frac{dp_T}{dt} = 0$, thus fraction of QDs capturing holes is given by

$$\frac{p_T}{N_{QD}} = \frac{1}{1 + \left(\frac{C_n n}{C_p p}\right)}. \tag{3}$$

At this stage, we take note of two distinct possibilities. The observed QD concentration dependence can be attributed either to the ratio of capture-coefficients $\left(\frac{C_n}{C_p}\right)$, or to the ratio of carrier concentrations $\left(\frac{n}{p}\right)$ As for the carrier concentrations, the p concentration is kept the same experimentally. Any dependence on electron concentration would be highly temperature dependent through the electron quasi-Fermi level. As argued earlier, since the exponential growth coefficient is nearly temperature independent, we are led to the conclusion that the ratio of capture coefficients is responsible in this case. We introduce the assumption that the hole capture cross-section is exponentially distributed such that $C_p = C_{p_o} e^{V_c N_{QD}}$ so that Eq. (3) can be rewritten as

$$\frac{p_T}{N_{QD}} = \frac{1}{1 + \left(\frac{C_n n}{C_{p_o} p}\right) e^{-V_c N_{QD}}}. \tag{4}$$

This can now be compared to the empirical form of QD concentration dependence $P_{emission}$ obtained in Eq. (1)

giving rise to the sigmoidal functional form. The parameter α would then correspond to $\frac{C_n n}{C_{p_o} p}$ From the point of view of energetics, C_n is likely to be more than C_{p_o}, and hence α would expected to be a large number as observed in our empirical fits. Ignoring unity as compared to the second term in the denominator in Eq. (4), the steady state recombination current density then becomes directly proportional to the exponential dependence of the hole capture cross-section.

$$\frac{p_T}{N_{QD}} \simeq \frac{C_{p_o}}{C_n}\left(\frac{p}{n}\right)e^{V_c N_{QD}}. \tag{5}$$

This provides a compelling rationale for our analysis in the last section. Thus, to summarize, the phenomenological model is able to mimic Eq. (1), and has two key attributes: (i) the emission at QD is assumed to occur when a hole is captured at a negatively charged QD, and (ii) the hole capture cross-section is distributed since non-uniform spatial distribution of QDs can lead to cluster-like region of different sizes. We go on to discuss possible origin of the large capture cross-section and its concentration dependence in the next section.

3.4. Possible origin of capture mechanism

Our results demonstrate the crucial difference between the concentration dependence of EL and PL. The fact that PL shows linear dependence with QD concentration indicates that it is directly proportional to the probability of an exciton reaching a QD recombination site. If the inter-particle distance in the composite is more than the exciton diffusion length, it would be insensitive to the particle distribution. The probability of recombination in such a case is expected to change linearly, which can be also considered as an approximation to a Poisson process with a very low probability of capture.

In contrast, the capture cross-section dependence measured for EL suggests that the capture mechanism is a long range interaction of Coulombic or dipolar origin. The long range interaction becomes sensitive to particle density distribution within the sampled volume since the inter-particle distance is much smaller. The measured capture cross-section distribution tells us that colonies of particles with 40 nm radius are the most effective average size for capture. We indeed do observe such colonies which are not aggregates and maintain an inter-particle distance 3–5 nm. It is again significant to note here that in their recent work on polymers, Kuik et al. [31] infer hole capture coefficient (not capture cross-section) from fitting of intensity dependence of open circuit voltage under illumination. In the present study, the concentration dependence of trap recombination allows us to derive the spatial distribution of QD induced traps and hence the capture cross-section parameter of the Coulombic traps.

Since the EL capture cross-section is nearly temperature independent, the mechanism of carrier recombination cannot merely be described by a simple Coulomb process. If it were a Coulombic attraction between charges q_1 and q_2 at the QD site in a medium with effective relative dielectric constant ε_r, the critical radius for recombination r_c would be proportional to the temperature T as, $r_c = q_1 q_2/(4\pi\varepsilon_o\varepsilon_r k_B T)$, where ε_o and k_B are the permittivity of vacuum and Boltzmann constant, respectively. Hence an argument attributing increased capture radius to multiple charged QD sites would not be valid. This is not surprising in our model since it is the geometrical distribution of QDs in space that controls efficacy of capture. The CdSe QDs are known to be polarizable with a higher effective permittivity ($\varepsilon_r = 8$) [32] than the medium and would contribute to decreased radius of capture, if Frenkel excitons were involved as in PL. From the study of relaxation dynamics using pump–probe experiments, it is known that the yield of QD band-edge luminescence is poor since the process of relaxation of excited electron–hole pairs is inefficient due to 'phonon-bottleneck', i.e. non-availability of phonons of sufficient energy close to that of wider gaps between discrete states as a result of quantum confinement [33,34]. As for EL, the occurrence of a large capture cross-section, which is temperature insensitive from 10 K to 300 K, can be taken as the evidence that the process of capture of carriers is not phonon-limited. The holes getting captured must be shedding their extra energy through an efficient mechanism such as Auger relaxation, which is known to become more significant in QDs [35,36]. The relaxation of holes in QDs can be more efficient due to their large effective mass and hence narrower gaps between the states, and mixing of bands due to confinement. It is also possible that the inter-particle interaction among the QDs plays an important role in making the capture mechanism effective for the long range interaction involved in the process.

4. Conclusions

In summary, we have shown that mechanism of EL for embedded QDs is very different from that of PL. In electroluminescent devices made of host polymer PFO, the embedded CdSe/ZnS QDs of 3.2 nm diameter behave as giant capture centers with an exponentially distributed capture cross-section due to spatial distribution of the QDs. This leads to a nearly exponential increase of EL intensity with increase in QD concentration. The temperature dependence of EL intensity closely follows the carrier mobility showing that the radiative recombination is limited by velocity of the carrier, and a weak temperature dependence of the capture cross-section distribution shows that it is not limited by any energetic barrier or phonon-bottleneck. The long range interaction between carriers in EL makes it sensitive to the distribution of density of QDs, and in the particular case considered here, the colonies of QDs corresponding to capture cross-section are responsible for efficient capture. In contrast, the PL intensity increases linearly with QD concentration since the exciton diffusion length is less than the inter-particle distance, and the random distribution appears uniform to the excitons. We have proposed a capture model treating QDs as trapping centers whose capture cross-section is exponentially dependent on concentration due to non-uniform spatial distribution. It is important to reiterate

that these conclusions were possible since our measurements were carried out over a wide range of QD concentration under controlled conditions of fabrication, and possible ambiguities were avoided by keeping the impressed current density the same for all samples and temperatures. Our results and methodology will help to optimize the use of QDs in device design and the study of carrier relaxation in embedded quantum dots.

Acknowledgments

We thank Samtel Centre for Display Technologies, Indian Institute of Technology Kanpur, India for providing Class 1000 clean room equipped with advance processing and characterization facilities. We also thank to Council of Scientific and Industrial Research, New Delhi, and Department of Science and Technology, New Delhi, India for financial support (DST/R&D/20060243).

References

[1] D.V. Talapin, J.S. Lee, M.V. Kovalenko, E.V. Shevchenko, Chem. Rev. 110 (2010) 389.
[2] P. Reiss, E. Couderc, J.D. Girolamo, A. Pron, Nanoscale 3 (2011) 446.
[3] V.L. Colvin, M.C. Schlamp, A.P. Alivisatos, Nature 370 (1994) 354.
[4] B.O. Dabbousi, M.G. Bawendi, O. Onitsuka, M.F. Rubner, Appl. Phys. Lett. 66 (1995) 1316.
[5] H. Mattoussi, L.H. Radzilowski, B.O. Dabbousi, D.E. Fogg, R.R. Schrock, E.L. Thomas, M.F. Rubner, M.G. Bawendi, J. Appl. Phys. 86 (1999) 4390.
[6] H. Mattoussi, L.H. Radzilowski, B.O. Dabbousi, E.L. Thomas, M.G. Bawendi, M.F. Rubner, J. Appl. Phys. 83 (1998) 7965.
[7] M.C. Schlamp, X. Peng, A.P. Alivisatos, J. Appl. Phys. 82 (1997) 5837.
[8] N. Tessler, V. Medvedev, M. Kazes, S. Kan, U. Banin, Science 295 (2002) 1506.
[9] S. Coe, W.K. Woo, M.G. Bawendi, V. Bulović, Nature 420 (2002) 800.
[10] P.O. Anikeeva, C.F. Madigan, J.E. Halpert, M.G. Bawendi, V. Bulović, Phys. Rev. B 78 (2008) 085434.
[11] V. Wood, M.J. Panzer, D. Bozyigit, Y. Shirasaki, I. Rousseau, S. Geyer, M.G. Bawendi, V. Bulović, Nano Lett. 11 (2011) 2927.
[12] A.L. Rogach, Semiconductor Nanocrystal Quantum Dots: Synthesis Assembly, Spectroscopy and Applications, Springer, Wien: New York, 2008.
[13] Th. Förster, Ann. Phys. 437 (1948) 55.
[14] T.W.F. Chang, S. Musikhin, L. Bakueva, L. Levina, M.A. Hines, P.W. Cyr, E.H. Sargent, Appl. Phys. Lett. 84 (2004) 4295.
[15] M. Anni, L. Manna, R. Cingolani, D. Valerini, A. Cretí, M. Lomascolo, Appl. Phys. Lett. 85 (2004) 4169. Erratum: Appl. Phys. Lett. 88 (2006) 259901.
[16] Y. Li, A. Rizzo, R. Cingolani, G. Gigli, Adv. Materials 18 (2006) 2545.
[17] S. Kaufmann, T. Stöferle, N. Moll, R.F. Mahrt, U. Scherf, A. Tsami, D.V. Talapin, C.B. Murray, Appl. Phys. Lett. 90 (2007) 071108.
[18] P.T.K. Chin, R.A.M. Hikmet, R.A.J. Janssen, J. Appl. Phys. 104 (2008) 013108.
[19] T. Stöferle, U. Scherf, R.F. Mahrt, Nano Lett. 9 (1) (2009) 453.
[20] L. Yan, J.Y. Zhang, Y. Cui, Y. Qiao, Appl. Phys. Lett. 91 (2007) 243114.
[21] A.K. Tripathi, Ashish, Y.N. Mohapatra, Org. Electron. 11 (2010) 1753.
[22] I.H. Campbell, B.K. Crone, Appl. Phys. Lett. 92 (2008) 043303.
[23] S.L.M. van Mensfoort, R. Coehoorn, Phys. Rev. Lett. 100 (2008) 086802.
[24] J.R. Skalski, D.S. Robson, C.L. Matsuzaki, Ecol. Modell. 19 (1983) 299.
[25] S. Kotwicki, K.L. Weinberg, Alaska Fish. Res. Bull. 11 (2) (2005) 135.
[26] S.M. Sze, Physics of Semiconductor Devices, second ed., John Wiley and Sons, 1981 (Chapter 1, p. 35).
[27] H. Bässler, Phys. Status Solidi B 175 (1993) 15.
[28] R. Coehoorn, W.F. Pasveer, P.A. Bobbert, M.A.J. Michels, Phys. Rev. B 72 (2005) 155206.
[29] S.L.M. van Mensfoort, S.I.E. Vulto, R.A.J. Janssen, R. Coehoorn, Phys. Rev. B78 (2008) 085208.
[30] M. Bouhassoune, S.L.M. van Mensfoort, P.A. Bobbert, R. Coehoorn, Org. Electron. 10 (2009) 437.
[31] M. Kuik, L.J.A. Koster, G.A.H. Wetzelaer, P.W.M. Blom, Phys. Rev. Lett. 107 (2011) 256805.
[32] T.D. Krauss, L.E. Brus, Phys. Rev. Lett. 83 (1999) 4840.
[33] H. Benisty, C.M. Sotomayor-Torres, C. Weisbuch, Phys. Rev. B 44 (1991) 10945.
[34] V.I. Klimov, Nanocrystal Quantum Dots, second ed., CRC Press, 2010.
[35] U. Bockelmann, T. Egeler, Phys. Rev. B 46 (1992) 15574.
[36] A.L. Efros, V.A. Kharchenko, M. Rosen, Solid State Commun. 93 (1995) 281.